

Re-Mix: Optimizing Data Mixtures for Large Scale Imitation Learning

Anonymous Author(s)

Affiliation

Address

email

1 **Abstract:** Increasingly large imitation learning datasets are being collected with the
2 goal of training foundation models for robotics. However, despite the fact that data
3 selection has been of utmost importance in vision and natural language processing,
4 little work in robotics has questioned what data such models should actually be trained
5 on. In this work we investigate how to weigh different subsets or “domains” of robotics
6 datasets for robot foundation model pre-training. Concretely, we use distributionally
7 robust optimization (DRO) to maximize worst-case performance across all downstream
8 domains. Our method, Re-Mix, addresses the wide range of challenges that arise when
9 applying DRO to robotics datasets including variability in action spaces and dynamics
10 across different datasets. Re-Mix employs early stopping, action normalization, and
11 discretization to counteract these issues. Through extensive experimentation on the
12 largest open-source robot manipulation dataset, the Open X-Embodiment dataset, we
13 demonstrate that data curation can have an outsized impact on downstream performance.
14 Specifically, domain weights learned by Re-Mix outperform uniform weights by 38%
15 on average and outperform human-selected weights by 32% on datasets used to train
16 existing generalist robot policies, specifically the RT-X models.

17 **Keywords:** Data Curation, Data Quality, Robot Imitation Learning

18 1 Introduction

19 Many breakthroughs in machine learning can be attributed to “Internet-scale” datasets, from the
20 development of vision models like CLIP [1] to recent advancements in transformer-based language
21 modeling powered by the Common Crawl dataset [2]. Seeking to capitalize on this trend, several recent
22 efforts in robotics focus on collecting [3–6] or pooling [7] large scale robotics datasets with the goal of
23 training more performant imitation learning policies. Learning from this data, however, is particularly
24 challenging: robotics datasets are collected with different robots, environments, state spaces, action spaces,
25 and dynamics [8]. For example, the commonly used Bridge V2 Dataset [4] uses a third person camera
26 on a small WidowX robot and a cartesian delta control space, while many datasets [9–12] collected on
27 the popular and much larger Franka Panda robot use wrist cameras [3] or joint-space actions [13]. While
28 embracing such heterogeneity quickly scales the amount of available training data [7], it amplifies the
29 importance of a fundamental question: how do we curate these raw, heterogeneous data sources into
30 effective training datasets for generalist robot policies?

31 While early vision and language models were trained on highly-curated academic datasets such as ImageNet
32 [14], questions surrounding data selection have shaped modern training pipelines that use Internet-scale data
33 [15–17]. For example, the training of large language models involves numerous stages of data filtering [18].
34 Similarly large vision datasets, e.g., LAION [19], assess the quality of each data point using pre-trained
35 models such as CLIP [1]. Thus as scaling of robot datasets continues, we can expect robotics data curation to
36 become equally critical. Unfortunately, simple filtering techniques are often inadequate in robotics; we can-
37 not apply n-gram filters, and visual embeddings do not capture the sequential nature of episodic robot data.

38 Even though aspects of demonstration data such as action quality [20] and visual diversity [3, 4, 21] have
39 been shown to be of paramount importance to downstream performance, approaches for robotics data

40 curation remain limited. In imitation learning, the data selection problem has only been characterized
41 theoretically [22, 23] or in simple small-scale settings [24]. Thus in practice we are left with ad hoc
42 solutions. For example, though the Open-X-Embodiment dataset (OpenX) [7] is comprised of more
43 than 60 individual datasets totalling over 2M robot trajectories, the RT-X models released alongside it
44 were trained on a mixture of only 12 datasets, weighted based on expert intuition. The recently released
45 Octo [25] and OpenVLA [26] generalist policies were similarly trained on a subset of OpenX, where
46 the authors chose which datasets to include at what sampling weight based on a subjective notion of
47 “interestingness”. While the resulting data mixes are shown to work well in practice, their curation requires
48 extensive domain knowledge and manual data inspection. Such ad hoc selection strategies are unlikely
49 to scale to the rapidly growing datasets used to train robot policies [3, 5, 27].

50 In this work, we ask: how can we *automatically* curate large-scale robotics datasets to maximize perfor-
51 mance of generalist imitation learning policies across domains? Though many filtering techniques are not
52 directly applicable to robotics, we can borrow ideas from language modeling that systematically optimize
53 training data mixtures based on the model’s performance. Specifically, DoReMi [28] uses group distribu-
54 tionally robust optimization [29] to maximize the performance of a policy across all “domains” in a given
55 dataset. In the context of robotics, such “domains” can correspond to different scenes within a single dataset,
56 e.g., different toy kitchens when considering a data mixture from the Bridge V2 dataset [4], or can refer to
57 full robot datasets in the case of multi-dataset mixtures such as the OpenX dataset. However, due to the het-
58 erogeneity of robotics datasets we find that naively applying such techniques does not work. Distributionally
59 robust optimization approaches minimize worst-case loss. Differences in action spaces and their distribu-
60 tions can cause loss magnitudes to be imbalanced across domains, leading some domains to be weighed
61 more heavily than they should be. Moreover, the smaller size of robotics datasets makes overfitting easy.
62 Both of these issues result in poor estimates of model performance, and consequently bad mixture weights.

63 To address these problems, we propose Re-weighting Robotic Dataset Mixtures with Minimax Optimization
64 (Re-Mix for short), which instantiates the data curation problem as a min-max optimization, where a
65 policy *minimizes* its excess behavior cloning loss over a reference model subject to learned domain mixture
66 weights that try to *maximize* it. Intuitively, the excess loss measures how much room the policy has to
67 improve on a given domain, and the data mixture is optimized to maximize such improvement potential.
68 Crucially, we carefully control the loss magnitudes between domains via domain-independent action
69 normalization and discretization, even if the final policies we train are continuous diffusion models [30, 31].
70 Moreover, we find that selecting a reference model that has not overfit to any domain prevents drastic
71 skewing of the downstream domain weights.

72 We empirically evaluate Re-Mix by using it to automatically optimize the training data mixture for the
73 Bridge V2 dataset [4] and the OpenX-based dataset used to train RT-X [7]. We show that policies trained
74 with our data mix improve performance by 38% and 32% respectively over naïve data balancing and
75 human-expert-curated data mixtures in evaluations using WidowX and Franka robot arms. Additionally,
76 we show that weights from Re-Mix can effectively *sub-sample* both datasets, achieving competitive
77 performance when using only 25% of the original data, while using uniform or human curated weights
78 significantly reduces performance.

79 2 Related Work

80 In congruence with the rise of deep learning in various fields, data selection has become of increasing
81 interest. Here we review the most relevant works, organized by area.

82 **The Data Problem in Robotics.** Several recent works in robotics have focused on collecting large demon-
83 stration datasets for imitation learning in simulation [20, 32, 33] and the real world [3, 7, 34–38] to train
84 large-scale robot policies [6, 25, 39, 40]. Generally, these works along with others that study the influence
85 of data collection on compositional generalization [21, 41, 42] show that aspects of dataset construction
86 such as scene and task diversity have a direct impact on downstream policy generalization. Though several
87 studies focus on *how* data should be collected via specific hardware [43], collection procedures [11, 21, 44],
88 or provide theoretic insights about data collection [22], little work in robotics addresses the post-hoc dataset
89 selection and analysis problem. This is particularly important as the number and diversity of robot datasets
90 are increasing with less clear conclusions about how to train a policy that effectively consumes all the col-

91 lected data [3, 7, 25]. Baker et al. [45] train a classifier to predict data quality, but require human annotations
 92 which are impractical to scale. Perhaps most related are retrieval-based methods that subset datasets [12, 46],
 93 but do so based on a priori target task specifications and are thus inapplicable to training generalist policies.

94 **Data Curation in Computer Vision.** Computer vision datasets were originally hand-crafted and manually
 95 labeled [14, 47]. However, scaling datasets to beyond what is possible to curate by hand, while retaining
 96 quality, has been critical to increasing performance [1, 48]. Notably, filtering techniques based on
 97 metadata-count balancing [49], embeddings [19], optical flow [50], and clustering [51] have shown to
 98 greatly improve downstream performance despite filtering out large amounts of data. Though learning
 99 from demonstrations involves vision, at its core is *action* prediction and such techniques can only filter
 100 trajectories in an action-agnostic manner.

101 **Data Curation in Natural Language Processing.** When training on large real-world sources of text,
 102 language modeling pipelines employ a number of text-specific preprocessing steps [16, 18, 52, 53]. Other
 103 methods sub-set data to maximize downstream performance, but use techniques such as k-means clustering
 104 over embedded text [54, 55]. While such clustering techniques can potentially be visually informative in
 105 robotics they do not provide information about *actions*. Mixture techniques, such as Domain Reweighting
 106 with Minimax Optimization (DoReMi) [28] balance text domains using robust optimization and build
 107 upon ideas from prioritized training [56–58]. Our work is inspired by DoReMi as such robust optimization
 108 approaches can be applied to imitation learning as well. In this work, we discuss the challenges of applying
 109 these techniques in robotics, and propose a solution that addresses their limitations for effective dataset
 110 curation for imitation learning.

111 3 Re-weighting Robotic Dataset Mixtures with Minimax Optimization

112 In this section, we first formalize the problem of re-weighting robotics data mixtures for imitation learning.
 113 We then discuss our approach which uses distributionally robust optimization for selecting domain weights
 114 and sub-setting large robotics datasets.

115 **Problem Setup.** We consider the general imitation learning problem, where we are given a dataset of
 116 demonstrations $\mathcal{D} = \{\tau_1, \dots, \tau_n\}$ consisting of state-action trajectories $\tau = (s_1, a_1, \dots, s_{T_i}, a_{T_i})$. Our goal is
 117 to learn a parameterized policy π_θ that learns a mapping from states to actions $\pi_\theta: \mathcal{S} \rightarrow \mathcal{A}$. In practice, this
 118 is often done through standard imitation learning algorithms such as behavior cloning (BC) by minimizing
 119 the expected negative log-likelihood of the actions under the policy:

$$\mathcal{L}_{\text{BC}}(\pi_\theta, \mathcal{D}) = \mathbb{E}_{(s,a) \sim \mathcal{D}}[-\log \pi_\theta(a|s)] \quad (1)$$

120 However, datasets often contain more information than just state action pairs. We assume that the overall
 121 dataset \mathcal{D} can be split into k heterogeneous domains $\mathcal{D}_1, \dots, \mathcal{D}_k$. This is a general assumption: while
 122 these domains could be larger groups, like different datasets from the Open X-Embodiment dataset [7]
 123 with different embodiments, they could also be as small as single trajectories. Moreover, each of the k
 124 domains can differ in state space \mathcal{S} , action space \mathcal{A} , transition dynamics, or their distributions. In fact
 125 when learning large behavior models, such heterogeneity becomes necessary to access more sources of
 126 diverse data. In this work, we use the Bridge dataset [4] – with different environments as the domains,
 127 and the Open-X-Embodiment dataset [7] – with different robot embodiments as the differing domains.

128 Our goal is to learn a weighting vector $\alpha \in \Delta^k$ that specifies a probability distribution over all domains
 129 such that any model, when trained on a domain mixture weighted according to α , attains maximum
 130 performance *across all domains*. We note that unlike the data retrieval problem, which aims to curate data
 131 *for a particular target task*, our goal is to curate datasets for effective pre-training or co-training without
 132 any a priori knowledge of a target task.

133 **Distributionally Robust Optimization.** When pre-training on large amounts of robot data we want
 134 policies to *generalize* to new settings and tasks, not master a specific target task. With that in mind,
 135 we want to optimize for a data mixture that results in models that i) can perform as well as possible on
 136 each domain, but ii) do not overfit to any one domain at the expense of another. Distributionally robust
 137 optimization (DRO) techniques aim to solve the same problem: learn models that minimize the worst-case
 138 training loss [29] – BC loss in the case of imitation learning – across domains $\mathcal{D}_1 \dots \mathcal{D}_k$. Specifically,

139 naively applying group robust optimization techniques in robotics would result in the following objective:

$$\min_{\theta} \max_{\alpha \in \Delta^k} \sum_{i=1}^k \alpha_i \mathcal{L}_{\text{BC}}(\pi_{\theta}, \mathcal{D}_i). \quad (2)$$

140 With this objective, α up-weights domains that have a higher loss value, emphasizing the hardest domains.
 141 However, in practice we might not be interested in just fitting the domains with higher losses. For example,
 142 a robotics dataset with complex multi-modal rotation movements for bottle-cap unscrewing might always
 143 have higher BC loss than simple pick-place datasets. Thus, standard robust optimization techniques could
 144 end up ignoring the latter domain. Instead, as in prior work [28, 59, 60], we consider the *difference* in loss
 145 between our learned policy π_{θ} and a reference policy π_{ref} which is trained to convergence on an initial guess
 146 of the domain weights, usually assumed to be proportional to the size of each domain, i.e. uniform sampling
 147 of the data. In Eq. (2) this equates to replacing \mathcal{L}_{BC} with $\mathcal{L}_{\text{BC}}(\pi_{\theta}, \mathcal{D}_i) - \mathcal{L}_{\text{BC}}(\pi_{\text{ref}}, \mathcal{D}_i)$. We refer to this
 148 difference as the *excess loss*, and use it for robust optimization. Like before, this will down-weight domains
 149 that the policy fits well, as it can achieve a loss similar to that of the reference model. However, it crucially
 150 also down-weights domains which are difficult to fit (i.e. they have a high policy loss *and* a high reference
 151 loss) due to the relative nature of the excess loss. As an example, this can happen in the presence of
 152 sub-optimal actions. Therefore, only domains that have a high excess loss, meaning the policy can improve
 153 to match the reference model, will be up-weighted as α is chosen to maximize the excess overall loss.

154 Unfortunately, models learned directly using robust optimization often exhibit worse overall performance
 155 [61, 62], as they focus on minimizing *worst-case* loss instead of average loss. Alternatively, we can use
 156 the learned α vector for downstream training as in Xie et al. [28]. This gives us a set of reusable weights
 157 that can be used to train different policies without the need for robust optimization.

158 3.1 The Challenges of Applying Robust Optimization in Robotics

159 While Group DRO has been applied in language modeling [28], robust optimization techniques face
 160 unique challenges in robotics which we highlight here. We then detail how we adapt a distributionally
 161 robust optimization pipeline to select domain weights for robotics datasets.

162 **Unbalanced Losses.** Large robotics datasets are often highly hetero-
 163 geneous: many are collected across different embodiments, controllers,
 164 and frequencies. Even within the same dataset, different scenes or tasks
 165 require vastly different ranges and speeds of motion. As a result, some
 166 datasets may have an outsized effect on robust optimization. To address
 167 this issue, one needs to align action losses across domains. In our case, we apply Gaussian normalization
 168 to each domain *individually*. We note that bounds normalization [30] applied to each domain, would be
 169 insufficient as it would not align the moments of the action distributions.

170 To underline the importance of aligning actions to a common distribution, we construct a simple experiment
 171 by training a policy with Group DRO [29] (Eq. (2)) when the action distributions match versus when they
 172 differ. Specifically, we construct a *noise* domain where a subset of the Bridge V2 dataset [4] is assigned
 173 random Gaussian actions and a normal *bridge* domain which uses the original actions, either normalized
 174 to also be unit gaussian or rescaled between -1 and 1 using “bounds” normalization. When Gaussian
 175 normalization is applied to the *bridge* domain, the action distribution matches the random noise. When
 176 bounds normalization is applied, they do not. We show the learned domain weights α for each scheme
 177 in Table 1. While one might expect that α would correctly assign majority weight to the *bridge* domain
 178 since the *noise* domain is impossible for both the policy and reference model to fit, this is actually only true
 179 in the “Gaussian” case when the action distributions of both domains are aligned. When using “Bounds”
 180 normalization, the average action magnitude of the *bridge* domain is lower, and thus its losses are dwarfed
 181 by those of the *noise* domain.

182 **Continuous Losses.** Robust optimization has largely been applied in discrete classification problems
 183 with cross-entropy losses, for example in language modeling [60]. Popular policy learning approaches,
 184 however, often predict continuous actions and use L1 or L2 loss functions [20, 30, 63, 64]. Applying
 185 robust optimization in these settings can be problematic for two reasons. First, action distributions can
 186 be multi-modal, and expressive continuous policy classes such as diffusion models only optimize an

	α^{noise}	α^{bridge}
Bounds	0.943	0.057
Gaussian	0.158	0.842

Table 1: Learned α from toy setting in Section 3.1

187 upper bound on the true loss. DRO techniques depend on estimating the true loss of each domain to
 188 weight different domains, and upper-bounds may not uniformly converge across domains resulting in
 189 inaccurate domain weights. Moreover, computing diffusion policy’s upper bound is expensive as it requires
 190 losses at every time-step in the diffusion process. However, without the expressiveness to fit multi-modal
 191 distributions, both the reference policy and DRO would be unable to effectively minimize BC loss on
 192 domains with multi-modal actions. Second, compared to language datasets, robot datasets often have a
 193 large number of action outliers which can heavily sway the value of continuous action losses. With L1 or
 194 L2 loss, these outliers can significantly increase the loss of a given domain, causing DRO to believe it can
 195 still make progress on the domain, causing it to be up-weighted. To resolve these problems, when applying
 196 robust optimization in the robotics domain, we discretize each action dimension via binning.

197 **Overfitting.** Datasets in language modeling often contain billions of tokens. As a result, robust
 198 optimization techniques like Xie et al. [28] do not experience overfitting when applied to these large scale
 199 datasets. On the other hand, large robot datasets are comparatively small (~ 10 -100k demonstrations).
 200 Moreover, individual datasets in mixtures like the Open X-Embodiment dataset [7] can be as small
 201 as 100 demonstrations. This is problematic when using the excess loss for robust optimization: if the
 202 reference model can achieve near-zero training loss on every data point within a domain, the excess loss is
 203 equivalent to the regular loss (since the reference loss is always $\simeq 0$) and α no longer reflects the potential
 204 for improvement on each domain. To counteract this problem, we employ aggressive early stopping on
 205 both the reference model and robust optimization. Specifically, we select the latest checkpoint from the
 206 reference model that has not overfit to *any* of the domains $\mathcal{D}_1, \dots, \mathcal{D}_k$ as measured by the difference in
 207 loss values between the training dataset and a held-out validation dataset for the respective domain.

208 3.2 Re-weighting Robotic Dataset Mixtures with Minimax Optimization

209 Our approach, Re-Mix, uses group distributional robustness to determine the weights of a data mixture
 210 [28] that could then be used for policy training and incorporates the key design considerations from the
 211 previous section, addressing issues around unbalanced losses, continuous losses, and overfitting. We note
 212 that Re-Mix only returns the weights of the data mixture α , as opposed to the final policy. This is to
 213 decouple the data curation problem from the policy training problem. After running Re-Mix, the resulting
 214 weights can be used for learning policies of a different type (i.e. diffusion) or at a larger scale.

215 **Stage 1: Action Preprocessing.** Following Section 3.1, we apply Gaussian normalization separately to
 216 every domain \mathcal{D}_k with different action spaces and dynamics, and then discretize actions via binning.

217 **Stage 2: Reference Model Training.** Next, we train a discrete reference model π_{ref} on the uniform mixture
 218 of domains $\mathcal{D}_1, \dots, \mathcal{D}_k$, where each domain is weighted in proportion to its size. We select the final reference
 219 model checkpoint by validation loss per Section 3.1, and use it to estimate the excess loss per domain.

220 **Stage 3: Group Distributionally Robust Optimization.** We learn the domain weights α via the following
 221 robust optimization with a discrete policy π_θ :

$$\min_{\theta} \max_{\alpha \in \Delta^k} \sum_{i=1}^k \alpha_i \left[\frac{1}{|\mathcal{D}_i|} \sum_{(s,a) \in \mathcal{D}_i} (-\log \pi_\theta(a|s) + \log \pi_{\text{ref}}(a|s)) \right], \quad (3)$$

222 which minimizes the worst case excess BC loss of the learned policy $-\log \pi_\theta(a|s) + \log \pi_{\text{ref}}(a|s)$ over
 223 all possible weightings of the domains $\alpha \in \Delta^k$. To update α , following [29], we perform one step of
 224 exponentiated gradient ascent on α followed by domain-weighted gradient descent on θ at each training
 225 step. Our resulting values of α upweight domains that we can still improve on, while downweighting
 226 domains that are trivial or impossible to fit. This means that Re-Mix directly filters data based on actions,
 227 unlike other techniques in vision and language that solely filter based on embeddings [55, 65]. We
 228 optimized Eq. (3) for the same number of steps as the reference model.

229 **Stage 4: Data Weighting for Policy Training.** After our robust optimization stage over the excess loss, we
 230 take the average value of α over the course of training, which we denote by $\bar{\alpha}$. We can then use this value
 231 of $\bar{\alpha}$ to re-weight different domains, or even subset datasets. In practice, this means that we can re-use
 232 the weights for several training runs with different configurations. For example, Re-Mix uses discrete
 233 actions, but we train final policies with diffusion which has shown to perform well empirically [25, 30].

234 4 Experiments

235 We aim to answer the following questions: (1) Does Re-Mix effectively curate large robot datasets for down-
236 stream policy learning? (2) Can we use Re-Mix to heavily sub-sample robot datasets while retaining good
237 performance? (3) Which design decisions matter for effective automatic curation of large robot datasets?

238 4.1 Experimental Setup

239 **Datasets.** We test Re-Mix curation on two widely-used, large-scale robot datasets: (1) the Bridge V2
240 Dataset [4], consisting of 50k diverse teleoperated demonstrations of single-arm manipulation tasks with a
241 WidowX 6 DoF robot arm, and (2) the datasets from the Open X-Embodiment dataset used to train RT-1-X
242 and RT-2-X models [7] which have third-person cameras, consisting of a total of 350k demonstrations
243 which span disparate embodiments and environments. We use “RT-X” to refer to this set of datasets. We
244 partition the Bridge V2 dataset into 32 domains based on the scenes the data was collected in. For OpenX,
245 we use each of the 11 datasets in the RT-X training set as domains. For a detailed list of all datasets and
246 partitions, see Appendix B. For simulation experiments in RoboMimic, see Appendix A.

247 **Training and Evaluation Details.** We aim to assess the quality of
248 various curated pre-training data mixtures for downstream policy learn-
249 ing. To that end, we co-train generalist goal-conditioned policies on the
250 curated datasets. As we do not have access to the robot setups used
251 to collect the datasets we train on, we construct our own WidowX and
252 Franka robot evaluation setups. Unfortunately, policies trained on *only* the
253 pre-training data failed to zero-shot generalize to our out-of-distribution
254 setups. To address this, we follow prior works [3, 12, 46, 66] and co-train
255 our policies on a small amount of in-domain data (25 demonstrations
256 each for 3 representative tasks), added to the final training mixture at a
257 small weight of 5%. We then evaluate policies on tasks that are out-of-
258 distribution with respect to the co-training data to test generalization. As a
259 result of co-training, all policies achieve non-zero success rate. However,
260 we note that the in-domain dataset is small enough that the quality of the
261 pre-training data mix still has significant impact on the evaluation result, providing a good test bed for data
262 curation approaches. All models are evaluated in the real world with 10 trials per task totaling over 500
263 real-world trials cumulatively. For all policies we use a ResNet 50 image encoder [67]. For the Re-Mix
264 reference model and Group DRO optimization, we use a discrete MLP action head. For all final policies
265 we use the diffusion head from [4, 25, 68] and train all models for 400,000 gradient steps.

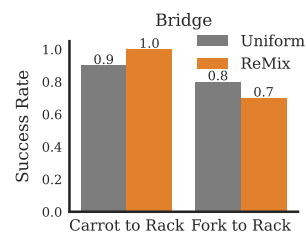


Figure 1: On Bridge V2 [4] there is no notable difference between uniform sampling vs. Re-Mix when training on the full dataset.

266 **Comparisons.** We compare the quality of Re-Mix’s curated data mixes to a naïve baseline: sampling
267 uniformly from each domain according to the total number of state-action pairs (**Uniform**). For evaluations
268 on the OpenX datasets, we additionally compare to a human-expert-curated data mix, using the hand-crafted
269 weights from RT-X [7]. For Bridge there is no expert-curated data mix — uniform sampling is the norm.

270 4.2 How do Re-Mix weights impact performance?

271 In Fig. 2, we show results for weighing datasets from the RT-X mix according to different methods. For
272 the WidowX robot, we consider four tasks that test generalization to 1) unseen objects: “Carrot to Rack”,
273 “OOD Cup”, 2) unseen initial conditions: “Fork to Rack”, and 3) distractors at the goal location “Cube to
274 Plate”. Similarly, for the Franka Panda robot we consider two tasks that test generalization to 1) unseen
275 initial conditions “Pen in Cup” and 2) motions not seen in the RT-X data “Flip Bowl”. Additionally, our
276 Panda robot uses a Robotiq 2F-85 gripper, which was not present in any of the RT-X-datasets. Note that for
277 the RT-X mix, we co-train the same model on both the WidowX and Franka data. As expected, we find
278 that the domain weights selected by human experts for the RT-X models outperform the naïve uniform
279 sampling baseline by 6% on average. More interestingly, we find that weighting datasets according to
280 Re-Mix outperforms uniform weighting by 38% on average, and surprisingly outperforms the human
281 curated weights by 32% on average. Fig. 1 shows results using Re-Mix weights versus uniform weighting
282 over scenes in the Bridge dataset. We find that performance in this setting is similar across both models.

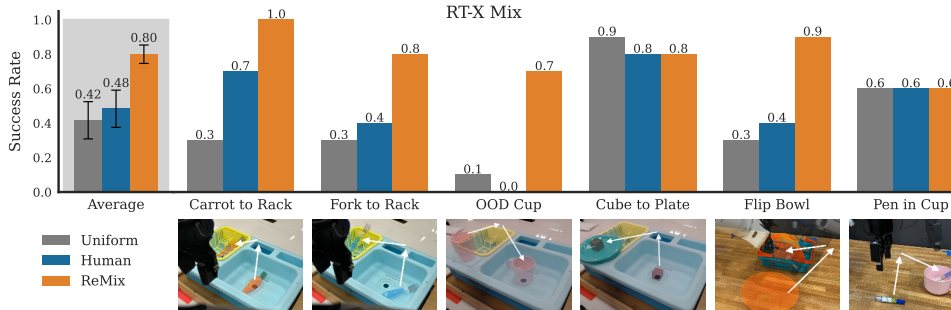


Figure 2: Results for curating the RT-X training mix. We test policies trained on different weightings of the data mixture used by RT-X across two WidowX (left) and two Franka (right) tabletop manipulation tasks. We find that the policy trained on the data mix curated with Re-Mix achieves strongest performance, even outperforming the human-expert-curated data mix from RT-X [7]. Mean \pm StdErr across 4 tasks, 10 evaluations each.

Method	α_{UR5}	$\alpha_{Cable Routing}$	α_{Bridge}	α_{Jaco}	α_{Kuka}	$\alpha_{RoboTurk}$	α_{RT1}	$\alpha_{Taco Play}$	$\alpha_{Taco Extra}$	α_{Toto}	α_{Viola}
Uniform	1.01%	0.43%	22.7%	0.81%	24.9%	1.94%	40.9%	0.60%	2.46%	3.42%	0.80%
Human	1.22%	1.56%	27.5%	1.95%	25.1%	2.35%	26.8%	1.46%	5.94%	4.13%	1.90%
Re-Mix	2.37%	0.20%	19.9%	0.39%	12.1%	1.14%	42.5%	0.63%	3.04%	16.3%	1.51%

Table 2: Dataset mixture weights by different methods on the RT-X dataset mix [4, 6, 9, 10, 37, 69–72]. We color relative increases of more than 25% from uniform green and relative decreases of more than 25% red.

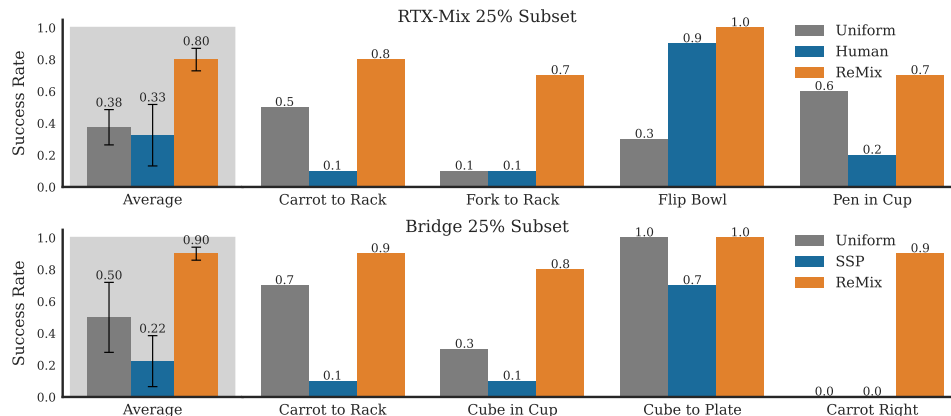


Figure 3: Results sub-setting datasets via different strategies until they reach 25% of their original size. We again use 10 evaluations per task, and show the Mean \pm StdErr.

283 We posit that in the presence of the full Bridge dataset, selecting weightings is less important as the model
 284 is able to fit every scene well.

285 4.3 Analyzing Re-Mix Weights

286 **Table 2** shows the weights produced by different methods on the RT-X dataset mix in comparison to the uni-
 287 form mixture, which corresponds to sampling each datapoint with equal probability or equivalently weight-
 288 ing each domain by its total size (as fraction of the total number of datapoints). The human-expert-designed
 289 weights largely down-weight RT-1 [6], while up-weighting some of the smaller datasets like Routing [69],
 290 and Taco [9], perhaps to ensure they were sampled often enough to not be ignored. On the other hand, Re-
 291 Mix largely down-weights the Kuka dataset [72]. This dataset was autonomously collected and then filtered
 292 by success, making it of potentially lower action quality. Re-Mix also down-weights some smaller domains
 293 that are easy to fit; for example, Cable Routing has no gripper actions and Jaco [70] only has three possible
 294 actions. Surprisingly, Re-Mix up-weights the Toto dataset [73] by more than 4x. We posit that this is because
 295 Toto has a particularly multi-modal action distribution which deviates far from a standard Gaussian even after
 296 normalization and thus may be more challenging to fit. See [Appendix A](#) for a plot of its action distribution.

297 4.4 How well does Re-Mix subset datasets?

298 Though co-training on diverse data is important for performance [3, 66], doing so is often expensive given
 299 that modern robot datasets like the Open X-Embodiment dataset encompass TBs of data. In this section, we

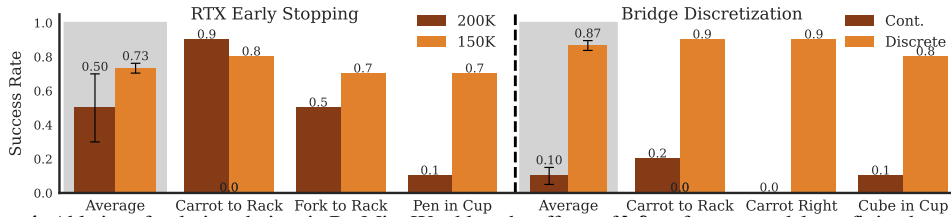


Figure 4: Ablations for design choices in Re-Mix. We ablate the effects of **left:** reference model overfitting by selecting a checkpoint once validation loss starts increasing at 150K steps and **right:** using continuous actions for Re-Mix. For ablations, we remove the “Flip Bowl” and “Cube to Plate” tasks as all Re-Mix variants achieved 100% success.

300 evaluate how well Re-Mix can be used to *subset* datasets. The key idea: if Re-Mix weights are proportional
 301 to the importance of the data in each domain, we can use them to effectively sub-set the dataset by removing
 302 data from domains that Re-Mix assigns low weight. We subset the base datasets according to Re-Mix and
 303 baselines by first computing the target size of the entire data mix *after* sub-setting, in our case 25% of $|\mathcal{D}|$.
 304 Then, we remove datapoints according to the mixture weights $\bar{\alpha}$.

305 Here, we compare performance of Re-Mix to using naïve uniform sampling for subsetting, and to subsetting
 306 based on the human expert weights. For Bridge, where no expert weighting exists, we additionally compare
 307 to a vision and language subsetting method called “Self-Supervised Prototypes” (SSP) [65] which runs
 308 k-means on image embeddings and discards data closest to each centroid to encourage diversity. We
 309 average CLIP embeddings across each trajectory to obtain the embeddings for k-means and use $k = 32$
 310 to match the number of domains used by Re-Mix. To provide a more extensive evaluation on Bridge,
 311 we add two additional tasks. “Cube in Cup” requires a different motion and a more precise place and
 312 “Carrot to Right”, which requires the robot to move the unseen carrot object to the right evaluates a motion
 313 unseen in the co-training data.

314 Our subsetting results can be found in Fig. 3. Overall, we find that subsetting exacerbates the difference
 315 between methods, as the weights now directly affect dataset composition. On the four evaluation tasks used
 316 for subsetting, Re-Mix, human, and uniform weighting had an average success rate of 82.5%, 52.5%, and
 317 37.5% on the four evaluation tasks used for subsetting. On the RT-X datasets (Fig. 3 top row) with only
 318 25% of the data Re-Mix retains performance, losing only 2.5% success rate while human weights drop
 319 over 10%. This is likely because as shown in Table 2 Re-Mix places higher weights on some of the smaller
 320 datasets and down-weights some of the larger datasets such as the Kuka dataset from [40]. On Bridge
 321 (Fig. 3 bottom row), Re-Mix also outperforms baseline methods. Overall SSP performs poorly, likely since
 322 robot trajectories may be out-of-distribution for vision models such as CLIP, causing the k-means clustering
 323 to be uncorrelated with data diversity.

324 4.5 What matters in Re-Mix?

325 In this section, we ablate several design choices used in Re-Mix (see Section 3.1), including action
 326 discretization and early stopping. We run all ablations in the 25% subset setting (see Section 4.4), since
 327 subsetting further amplifies the effects of the domain weights. In Fig. 4, we first analyze the effects of
 328 choosing a reference model checkpoint for Group DRO that is overfit to the training dataset. Empirically,
 329 we find that choosing a checkpoint just 50K steps after early stopping decreases performance by over
 330 15% on average, likely because the reference model baseline used to determine the domain weights is
 331 less meaningful once it overfits. On the right half of Fig. 4, we show performance on Bridge when using
 332 continuous (Cont.) actions in Re-Mix instead of discrete for estimating α . We find that continuous
 333 lead to significantly worse performance, as their loss functions fail to fit outliers or multi-modal actions.

334 5 Conclusion

335 In this work we present Re-Mix, a method for automatically curating robotics datasets using distributionally
 336 robust optimization. We find that Re-Mix can generate dataset mixes that outperform both uniform and
 337 human-curated weights on the challenging RT-X data mix, even when subsetting datasets to 25% of their
 338 original scale.

339 **References**

340 [1] A. Radford, J. W. Kim, C. Hallacy, A. Ramesh, G. Goh, S. Agarwal, G. Sastry, A. Askell, P. Mishkin,
341 J. Clark, et al. Learning transferable visual models from natural language supervision. In *International*
342 *conference on machine learning*, pages 8748–8763. PMLR, 2021.

343 [2] A. Conneau, K. Khandelwal, N. Goyal, V. Chaudhary, G. Wenzek, F. Guzmán, E. Grave, M. Ott,
344 L. Zettlemoyer, and V. Stoyanov. Unsupervised cross-lingual representation learning at scale. *arXiv*
345 *preprint arXiv:1911.02116*, 2019.

346 [3] A. Khazatsky, K. Pertsch, S. Nair, A. Balakrishna, S. Dasari, S. Karamcheti, S. Nasiriany, M. K.
347 Srirama, L. Y. Chen, K. Ellis, et al. Droid: A large-scale in-the-wild robot manipulation dataset.
348 *arXiv preprint arXiv:2403.12945*, 2024.

349 [4] H. Walke, K. Black, A. Lee, M. J. Kim, M. Du, C. Zheng, T. Zhao, P. Hansen-Estruch, Q. Vuong,
350 A. He, V. Myers, K. Fang, C. Finn, and S. Levine. Bridgedata v2: A dataset for robot learning at
351 scale. In *Conference on Robot Learning (CoRL)*, 2023.

352 [5] H.-S. Fang, H. Fang, Z. Tang, J. Liu, J. Wang, H. Zhu, and C. Lu. Rh20t: A robotic dataset for
353 learning diverse skills in one-shot. In *RSS 2023 Workshop on Learning for Task and Motion Planning*,
354 2023.

355 [6] A. Brohan, N. Brown, J. Carbajal, Y. Chebotar, J. Dabis, C. Finn, K. Gopalakrishnan, K. Hausman,
356 A. Herzog, J. Hsu, J. Ibarz, B. Ichter, A. Irpan, T. Jackson, S. Jesmonth, N. Joshi, R. Julian,
357 D. Kalashnikov, Y. Kuang, I. Leal, K.-H. Lee, S. Levine, Y. Lu, U. Malla, D. Manjunath, I. Mordatch,
358 O. Nachum, C. Parada, J. Peralta, E. Perez, K. Pertsch, J. Quiambao, K. Rao, M. Ryoo, G. Salazar,
359 P. Sanketi, K. Sayed, J. Singh, S. Sontakke, A. Stone, C. Tan, H. Tran, V. Vanhoucke, S. Vega,
360 Q. Vuong, F. Xia, T. Xiao, P. Xu, S. Xu, T. Yu, and B. Zitkovich. Rt-1: Robotics transformer for
361 real-world control at scale. In *arXiv preprint arXiv:2212.06817*, 2022.

362 [7] Open X-Embodiment Collaboration, A. Padalkar, A. Pooley, A. Jain, A. Bewley, A. Herzog, A. Irpan,
363 A. Khazatsky, A. Rai, A. Singh, A. Brohan, A. Raffin, A. Wahid, B. Burgess-Limerick, B. Kim,
364 B. Schölkopf, B. Ichter, C. Lu, C. Xu, C. Finn, C. Xu, C. Chi, C. Huang, C. Chan, C. Pan, C. Fu,
365 C. Devin, D. Driess, D. Pathak, D. Shah, D. Büchler, D. Kalashnikov, D. Sadigh, E. Johns, F. Ceola,
366 F. Xia, F. Stulp, G. Zhou, G. S. Sukhatme, G. Salhotra, G. Yan, G. Schiavi, H. Su, H.-S. Fang,
367 H. Shi, H. B. Amor, H. I. Christensen, H. Furuta, H. Walke, H. Fang, I. Mordatch, I. Radosavovic,
368 I. Leal, J. Liang, J. Kim, J. Schneider, J. Hsu, J. Bohg, J. Bingham, J. Wu, J. Luo, J. Gu,
369 J. Tan, J. Oh, J. Malik, J. Tompson, J. Yang, J. J. Lim, J. Silvério, J. Han, K. Rao, K. Pertsch,
370 K. Hausman, K. Go, K. Gopalakrishnan, K. Goldberg, K. Byrne, K. Oslund, K. Kawaharazuka,
371 K. Zhang, K. Majd, K. Rana, K. Srinivasan, L. Y. Chen, L. Pinto, L. Tan, L. Ott, L. Lee, M. Tomizuka,
372 M. Du, M. Ahn, M. Zhang, M. Ding, M. K. Srirama, M. Sharma, M. J. Kim, N. Kanazawa, N. Hansen,
373 N. Heess, N. J. Joshi, N. Suenderhauf, N. D. Palo, N. M. M. Shafiullah, O. Mees, O. Kroemer,
374 P. R. Sanketi, P. Wohlhart, P. Xu, P. Sermanet, P. Sundareshan, Q. Vuong, R. Rafailov, R. Tian,
375 R. Doshi, R. Martín-Martín, R. Mendonca, R. Shah, R. Hoque, R. Julian, S. Bustamante, S. Kirmani,
376 S. Levine, S. Moore, S. Bahl, S. Dass, S. Song, S. Xu, S. Haldar, S. Adebola, S. Guist, S. Nasiriany,
377 S. Schaal, S. Welker, S. Tian, S. Dasari, S. Belkhale, T. Osa, T. Harada, T. Matsushima, T. Xiao,
378 T. Yu, T. Ding, T. Davchev, T. Z. Zhao, T. Armstrong, T. Darrell, V. Jain, V. Vanhoucke, W. Zhan,
379 W. Zhou, W. Burgard, X. Chen, X. Wang, X. Zhu, X. Li, Y. Lu, Y. Chebotar, Y. Zhou, Y. Zhu,
380 Y. Xu, Y. Wang, Y. Bisk, Y. Cho, Y. Lee, Y. Cui, Y. hua Wu, Y. Tang, Y. Zhu, Y. Li, Y. Iwasawa,
381 Y. Matsuo, Z. Xu, and Z. J. Cui. Open X-Embodiment: Robotic learning datasets and RT-X models.
382 <https://arxiv.org/abs/2310.08864>, 2023.

383 [8] J. H. Yang, D. Sadigh, and C. Finn. Polybot: Training one policy across robots while embracing
384 variability. In *7th Annual Conference on Robot Learning*, 2023. URL [https://openreview.net/](https://openreview.net/forum?id=HEIRj51lcS)
385 [forum?id=HEIRj51lcS](https://openreview.net/forum?id=HEIRj51lcS).

- 386 [9] E. Rosete-Beas, O. Mees, G. Kalweit, J. Boedecker, and W. Burgard. Latent plans for task agnostic
387 offline reinforcement learning. In *Proceedings of the 6th Conference on Robot Learning (CoRL)*,
388 2022.
- 389 [10] Y. Zhu, A. Joshi, P. Stone, and Y. Zhu. Viola: Imitation learning for vision-based manipulation with
390 object proposal priors. *6th Annual Conference on Robot Learning (CoRL)*, 2022.
- 391 [11] S. Belkhale, Y. Cui, and D. Sadigh. Hydra: Hybrid robot actions for imitation learning. In *Conference*
392 *on Robot Learning*, pages 2113–2133. PMLR, 2023.
- 393 [12] S. Nasiriany, T. Gao, A. Mandlekar, and Y. Zhu. Learning and retrieval from prior data for skill-based
394 imitation learning. In *Conference on Robot Learning (CoRL)*, 2022.
- 395 [13] H. Bharadhwaj, J. Vakil, M. Sharma, A. Gupta, S. Tulsiani, and V. Kumar. Roboagent: Generalization
396 and efficiency in robot manipulation via semantic augmentations and action chunking, 2023.
- 397 [14] J. Deng, W. Dong, R. Socher, L.-J. Li, K. Li, and L. Fei-Fei. Imagenet: A large-scale hierarchical
398 image database. In *2009 IEEE Conference on Computer Vision and Pattern Recognition*, pages
399 248–255, 2009. doi:10.1109/CVPR.2009.5206848.
- 400 [15] L. Gao, S. Biderman, S. Black, L. Golding, T. Hoppe, C. Foster, J. Phang, H. He, A. Thite,
401 N. Nabeshima, S. Presser, and C. Leahy. The Pile: An 800gb dataset of diverse text for language
402 modeling. *arXiv preprint arXiv:2101.00027*, 2020.
- 403 [16] G. Penedo, H. Kydlíček, L. von Werra, and T. Wolf. Fineweb, April 2024. URL [https://](https://huggingface.co/datasets/HuggingFaceFW/fineweb)
404 huggingface.co/datasets/HuggingFaceFW/fineweb.
- 405 [17] K. Grauman, A. Westbury, E. Byrne, Z. Chavis, A. Furnari, R. Girdhar, J. Hamburger, H. Jiang,
406 M. Liu, X. Liu, et al. Ego4d: Around the world in 3,000 hours of egocentric video. In *Proceedings of*
407 *the IEEE/CVF Conference on Computer Vision and Pattern Recognition*, pages 18995–19012, 2022.
- 408 [18] A. Albalak, Y. Elazar, S. M. Xie, S. Longpre, N. Lambert, X. Wang, N. Muennighoff, B. Hou, L. Pan,
409 H. Jeong, C. Raffel, S. Chang, T. Hashimoto, and W. Y. Wang. A survey on data selection for
410 language models, 2024.
- 411 [19] C. Schuhmann, R. Beaumont, R. Vencu, C. Gordon, R. Wightman, M. Cherti, T. Coombes, A. Katta,
412 C. Mullis, M. Wortsman, et al. Laion-5b: An open large-scale dataset for training next generation
413 image-text models. *Advances in Neural Information Processing Systems*, 35:25278–25294, 2022.
- 414 [20] A. Mandlekar, D. Xu, J. Wong, S. Nasiriany, C. Wang, R. Kulkarni, L. Fei-Fei, S. Savarese, Y. Zhu,
415 and R. Martín-Martín. What matters in learning from offline human demonstrations for robot
416 manipulation. *arXiv preprint arXiv:2108.03298*, 2021.
- 417 [21] J. Gao, A. Xie, T. Xiao, C. Finn, and D. Sadigh. Efficient data collection for robotic manipulation via
418 compositional generalization, 2024.
- 419 [22] S. Belkhale, Y. Cui, and D. Sadigh. Data quality in imitation learning. *Advances in Neural Information*
420 *Processing Systems*, 36, 2024.
- 421 [23] S. Ross, G. Gordon, and D. Bagnell. A reduction of imitation learning and structured prediction
422 to no-regret online learning. In *Proceedings of the fourteenth international conference on artificial*
423 *intelligence and statistics*, pages 627–635. JMLR Workshop and Conference Proceedings, 2011.
- 424 [24] K. Gandhi, S. Karamcheti, M. Liao, and D. Sadigh. Eliciting compatible demonstrations for multi-
425 human imitation learning. In *Conference on Robot Learning*, pages 1981–1991. PMLR, 2023.
- 426 [25] Octo Model Team, D. Ghosh, H. Walke, K. Pertsch, K. Black, O. Mees, S. Dasari, J. Hejna, C. Xu,
427 J. Luo, T. Kreiman, Y. Tan, L. Y. Chen, P. Sanketi, Q. Vuong, T. Xiao, D. Sadigh, C. Finn, and
428 S. Levine. Octo: An open-source generalist robot policy. In *Proceedings of Robotics: Science and*
429 *Systems*, Delft, Netherlands, 2024.

- 430 [26] M. Kim, K. Pertsch, S. Karamcheti, T. Xiao, A. Balakrishna, S. Nair, R. Rafailov, E. Foster, G. Lam,
431 P. Sanketi, Q. Vuong, T. Kollar, B. Burchfiel, R. Tedrake, D. Sadigh, S. Levine, P. Liang, and C. Finn.
432 Openvla: An open-source vision-language-action model. *arXiv preprint arXiv:2406.09246*, 2024.
- 433 [27] S. Nasiriany, A. Maddukuri, L. Zhang, A. Parikh, A. Lo, A. Joshi, A. Mandlekar, and Y. Zhu.
434 Robocasa: Large-scale simulation of everyday tasks for generalist robots. In *Robotics: Science and
435 Systems (RSS)*, 2024.
- 436 [28] S. M. Xie, H. Pham, X. Dong, N. Du, H. Liu, Y. Lu, P. S. Liang, Q. V. Le, T. Ma, and
437 A. W. Yu. Doremi: Optimizing data mixtures speeds up language model pretraining. In
438 A. Oh, T. Naumann, A. Globerson, K. Saenko, M. Hardt, and S. Levine, editors, *Advances
439 in Neural Information Processing Systems*, volume 36, pages 69798–69818. Curran Asso-
440 ciates, Inc., 2023. URL [https://proceedings.neurips.cc/paper_files/paper/2023/
441 file/dcba6be91359358c2355cd920da3fcbd-Paper-Conference.pdf](https://proceedings.neurips.cc/paper_files/paper/2023/file/dcba6be91359358c2355cd920da3fcbd-Paper-Conference.pdf).
- 442 [29] S. Sagawa, P. W. Koh, T. B. Hashimoto, and P. Liang. Distributionally robust neural networks
443 for group shifts: On the importance of regularization for worst-case generalization. *arXiv preprint
444 arXiv:1911.08731*, 2019.
- 445 [30] C. Chi, S. Feng, Y. Du, Z. Xu, E. Cousineau, B. Burchfiel, and S. Song. Diffusion policy: Visuomotor
446 policy learning via action diffusion. In *Proceedings of Robotics: Science and Systems (RSS)*, 2023.
- 447 [31] M. Reuss, M. Li, X. Jia, and R. Lioutikov. Goal conditioned imitation learning using score-based
448 diffusion policies. In *Robotics: Science and Systems*, 2023.
- 449 [32] O. Mees, L. Hermann, E. Rosete-Beas, and W. Burgard. Calvin: A benchmark for language-
450 conditioned policy learning for long-horizon robot manipulation tasks. *IEEE Robotics and Automation
451 Letters (RA-L)*, 7(3):7327–7334, 2022.
- 452 [33] H. Ha, P. Florence, and S. Song. Scaling up and distilling down: Language-guided robot skill
453 acquisition. In *Proceedings of the 2023 Conference on Robot Learning*, 2023.
- 454 [34] E. Jang, A. Irpan, M. Khansari, D. Kappler, F. Ebert, C. Lynch, S. Levine, and C. Finn. Bc-z:
455 Zero-shot task generalization with robotic imitation learning. In *Conference on Robot Learning*,
456 pages 991–1002. PMLR, 2022.
- 457 [35] S. Dasari, F. Ebert, S. Tian, S. Nair, B. Bucher, K. Schmeckpeper, S. Singh, S. Levine, and C. Finn.
458 Robonet: Large-scale multi-robot learning. *arXiv preprint arXiv:1910.11215*, 2019.
- 459 [36] P. Sharma, L. Mohan, L. Pinto, and A. Gupta. Multiple interactions made easy (mime): Large scale
460 demonstrations data for imitation. In *Conference on robot learning*, pages 906–915. PMLR, 2018.
- 461 [37] A. Mandlekar, Y. Zhu, A. Garg, J. Booher, M. Spero, A. Tung, J. Gao, J. Emmons, A. Gupta, E. Orbay,
462 et al. Roboturk: A crowdsourcing platform for robotic skill learning through imitation. In *Conference
463 on Robot Learning*, pages 879–893. PMLR, 2018.
- 464 [38] L. Pinto and A. Gupta. Supersizing self-supervision: Learning to grasp from 50k tries and 700 robot
465 hours. In *2016 IEEE international conference on robotics and automation (ICRA)*, pages 3406–3413.
466 IEEE, 2016.
- 467 [39] B. Zitkovich, T. Yu, S. Xu, P. Xu, T. Xiao, F. Xia, J. Wu, P. Wohlhart, S. Welker, A. Wahid, et al. Rt-2:
468 Vision-language-action models transfer web knowledge to robotic control. In *Conference on Robot
469 Learning*, pages 2165–2183. PMLR, 2023.
- 470 [40] S. Levine, P. Pastor, A. Krizhevsky, J. Ibarz, and D. Quillen. Learning hand-eye coordination for
471 robotic grasping with deep learning and large-scale data collection. *The International journal of
472 robotics research*, 37(4-5):421–436, 2018.
- 473 [41] K. Burns, Z. Witzel, J. I. Hamid, T. Yu, C. Finn, and K. Hausman. What makes pre-trained visual
474 representations successful for robust manipulation? *arXiv preprint arXiv:2312.12444*, 2023.

- 475 [42] A. Xie, L. Lee, T. Xiao, and C. Finn. Decomposing the generalization gap in imitation learning for
476 visual robotic manipulation. *arXiv preprint arXiv:2307.03659*, 2023.
- 477 [43] S. Young, D. Gandhi, S. Tulsiani, A. Gupta, P. Abbeel, and L. Pinto. Visual imitation made easy. In
478 J. Kober, F. Ramos, and C. Tomlin, editors, *Proceedings of the 2020 Conference on Robot Learning*,
479 volume 155 of *Proceedings of Machine Learning Research*, pages 1992–2005. PMLR, 16–18 Nov
480 2021. URL <https://proceedings.mlr.press/v155/young21a.html>.
- 481 [44] M. Laskey, J. Lee, R. Fox, A. Dragan, and K. Goldberg. Dart: Noise injection for robust imitation
482 learning. In *Conference on robot learning*, pages 143–156. PMLR, 2017.
- 483 [45] B. Baker, I. Akkaya, P. Zhokov, J. Huizinga, J. Tang, A. Ecoffet, B. Houghton, R. Sampedro, and
484 J. Clune. Video pretraining (vpt): Learning to act by watching unlabeled online videos. *Advances in
485 Neural Information Processing Systems*, 35:24639–24654, 2022.
- 486 [46] M. Du, S. Nair, D. Sadigh, and C. Finn. Behavior retrieval: Few-shot imitation learning by querying
487 unlabeled datasets. *arXiv preprint arXiv:2304.08742*, 2023.
- 488 [47] A. Krizhevsky, G. Hinton, et al. Learning multiple layers of features from tiny images. 2009.
- 489 [48] M. Oquab, T. Darcet, T. Moutakanni, H. Vo, M. Szafraniec, V. Khalidov, P. Fernandez, D. Haziza,
490 F. Massa, A. El-Nouby, et al. Dinov2: Learning robust visual features without supervision. *arXiv
491 preprint arXiv:2304.07193*, 2023.
- 492 [49] H. Xu, S. Xie, X. Tan, P.-Y. Huang, R. Howes, V. Sharma, S.-W. Li, G. Ghosh, L. Zettlemoyer, and
493 C. Feichtenhofer. Demystifying CLIP data. In *The Twelfth International Conference on Learning
494 Representations*, 2024. URL <https://openreview.net/forum?id=5BCFlnfE1g>.
- 495 [50] A. Blattmann, T. Dockhorn, S. Kulal, D. Mendelevitch, M. Kilian, D. Lorenz, Y. Levi, Z. English,
496 V. Voleti, A. Letts, et al. Stable video diffusion: Scaling latent video diffusion models to large datasets.
497 *arXiv preprint arXiv:2311.15127*, 2023.
- 498 [51] H. V. Vo, V. Khalidov, T. Darcet, T. Moutakanni, N. Smetanin, M. Szafraniec, H. Touvron, C. Couprie,
499 M. Oquab, A. Joulin, et al. Automatic data curation for self-supervised learning: A clustering-based
500 approach. *arXiv preprint arXiv:2405.15613*, 2024.
- 501 [52] T. Computer. Redpajama: an open dataset for training large language models, October 2023. URL
502 <https://github.com/togethercomputer/RedPajama-Data>.
- 503 [53] L. Soldaini, R. Kinney, A. Bhagia, D. Schwenk, D. Atkinson, R. Authur, B. Bogin, K. Chandu,
504 J. Dumas, Y. Elazar, V. Hofmann, A. H. Jha, S. Kumar, L. Lucy, X. Lyu, N. Lambert, I. Magnusson,
505 J. Morrison, N. Muennighoff, A. Naik, C. Nam, M. E. Peters, A. Ravichander, K. Richardson, Z. Shen,
506 E. Strubell, N. Subramani, O. Tafjord, P. Walsh, L. Zettlemoyer, N. A. Smith, H. Hajishirzi, I. Beltagy,
507 D. Groeneveld, J. Dodge, and K. Lo. Dolma: An Open Corpus of Three Trillion Tokens for Language
508 Model Pretraining Research. *arXiv preprint*, 2024. URL <https://arxiv.org/abs/2402.00159>.
- 509 [54] K. Tirumala, D. Simig, A. Aghajanyan, and A. Morcos. D4: Improving llm pre-
510 training via document de-duplication and diversification. In A. Oh, T. Naumann,
511 A. Globerson, K. Saenko, M. Hardt, and S. Levine, editors, *Advances in Neu-
512 ral Information Processing Systems*, volume 36, pages 53983–53995. Curran Associates,
513 Inc., 2023. URL [https://proceedings.neurips.cc/paper_files/paper/2023/file/
514 a8f8cbd7f7a5fb2c837e578c75e5b615-Paper-Datasets_and_Benchmarks.pdf](https://proceedings.neurips.cc/paper_files/paper/2023/file/a8f8cbd7f7a5fb2c837e578c75e5b615-Paper-Datasets_and_Benchmarks.pdf).
- 515 [55] A. Abbas, K. Tirumala, D. Simig, S. Ganguli, and A. S. Morcos. Semdedup: Data-efficient learning
516 at web-scale through semantic deduplication, 2023.
- 517 [56] S. Mindermann, J. M. Brauner, M. T. Razzak, M. Sharma, A. Kirsch, W. Xu, B. Höltingen, A. N.
518 Gomez, A. Morisot, S. Farquhar, and Y. Gal. Prioritized training on points that are learnable, worth
519 learning, and not yet learnt. In K. Chaudhuri, S. Jegelka, L. Song, C. Szepesvari, G. Niu, and

- 520 S. Sabato, editors, *Proceedings of the 39th International Conference on Machine Learning*, volume
521 162 of *Proceedings of Machine Learning Research*, pages 15630–15649. PMLR, 17–23 Jul 2022.
522 URL <https://proceedings.mlr.press/v162/mindermann22a.html>.
- 523 [57] A. H. Jiang, D. L.-K. Wong, G. Zhou, D. G. Andersen, J. Dean, G. R. Ganger, G. Joshi, M. Kaminsky,
524 M. Kozuch, Z. C. Lipton, et al. Accelerating deep learning by focusing on the biggest losers. *arXiv*
525 *preprint arXiv:1910.00762*, 2019.
- 526 [58] M. Paul, S. Ganguli, and G. K. Dziugaite. Deep learning on a data diet: Finding important examples
527 early in training. *Advances in Neural Information Processing Systems*, 34:20596–20607, 2021.
- 528 [59] K. Chitta, J. M. Álvarez, E. Haussmann, and C. Farabet. Training data subset search with ensemble
529 active learning. *IEEE Transactions on Intelligent Transportation Systems*, 23(9):14741–14752, 2021.
- 530 [60] Y. Oren, S. Sagawa, T. B. Hashimoto, and P. Liang. Distributionally robust language modeling. In
531 *Proceedings of the 2019 Conference on Empirical Methods in Natural Language Processing and*
532 *the 9th International Joint Conference on Natural Language Processing (EMNLP-IJCNLP)*, pages
533 4227–4237, 2019.
- 534 [61] H. Zhang, Y. Yu, J. Jiao, E. Xing, L. El Ghaoui, and M. Jordan. Theoretically principled trade-off
535 between robustness and accuracy. In *International conference on machine learning*, pages 7472–7482.
536 PMLR, 2019.
- 537 [62] D. Tsipras, S. Santurkar, L. Engstrom, A. Turner, and A. Madry. Robustness may be at odds with
538 accuracy. *arXiv preprint arXiv:1805.12152*, 2018.
- 539 [63] T. Z. Zhao, V. Kumar, S. Levine, and C. Finn. Learning fine-grained bimanual manipulation with
540 low-cost hardware. *arXiv preprint arXiv:2304.13705*, 2023.
- 541 [64] F. Ebert, Y. Yang, K. Schmeckpeper, B. Bucher, G. Georgakis, K. Daniilidis, C. Finn, and S. Levine.
542 Bridge data: Boosting generalization of robotic skills with cross-domain datasets. *arXiv preprint*
543 *arXiv:2109.13396*, 2021.
- 544 [65] B. Sorscher, R. Geirhos, S. Shekhar, S. Ganguli, and A. Morcos. Beyond neural scaling laws: beating
545 power law scaling via data pruning. In S. Koyejo, S. Mohamed, A. Agarwal, D. Belgrave, K. Cho,
546 and A. Oh, editors, *Advances in Neural Information Processing Systems*, volume 35, pages 19523–
547 19536. Curran Associates, Inc., 2022. URL [https://proceedings.neurips.cc/paper_files/
548 paper/2022/file/7b75da9b61eda40fa35453ee5d077df6-Paper-Conference.pdf](https://proceedings.neurips.cc/paper_files/paper/2022/file/7b75da9b61eda40fa35453ee5d077df6-Paper-Conference.pdf).
- 549 [66] Z. Fu, T. Z. Zhao, and C. Finn. Mobile aloha: Learning bimanual mobile manipulation with low-cost
550 whole-body teleoperation. In *arXiv*, 2024.
- 551 [67] K. He, X. Zhang, S. Ren, and J. Sun. Deep residual learning for image recognition. In *Proceedings of*
552 *the IEEE Conference on Computer Vision and Pattern Recognition (CVPR)*, June 2016.
- 553 [68] P. Hansen-Estruch, I. Kostrikov, M. Janner, J. G. Kuba, and S. Levine. Idql: Implicit q-learning as an
554 actor-critic method with diffusion policies, 2023.
- 555 [69] J. Luo, C. Xu, X. Geng, G. Feng, K. Fang, L. Tan, S. Schaal, and S. Levine. Multi-stage cable routing
556 through hierarchical imitation learning. *arXiv pre-print*, 2023. URL [https://arxiv.org/abs/
557 2307.08927](https://arxiv.org/abs/2307.08927).
- 558 [70] S. Dass, J. Yapeter, J. Zhang, J. Zhang, K. Pertsch, S. Nikolaidis, and J. J. Lim. Clvr jaco play dataset,
559 2023. URL https://github.com/clvr-ai/clvr_jaco_play_dataset.
- 560 [71] L. Y. Chen, S. Adebola, and K. Goldberg. Berkeley UR5 demonstration dataset.
561 <https://sites.google.com/view/berkeley-ur5/home>.

- 562 [72] D. Kalashnikov, A. Irpan, P. Pastor, J. Ibarz, A. Herzog, E. Jang, D. Quillen, E. Holly, M. Kalakrishnan,
563 V. Vanhoucke, et al. Scalable deep reinforcement learning for vision-based robotic manipulation. In
564 *Conference on robot learning*, pages 651–673. PMLR, 2018.
- 565 [73] G. Zhou, V. Dean, M. K. Srirama, A. Rajeswaran, J. Pari, K. Hatch, A. Jain, T. Yu, P. Abbeel,
566 L. Pinto, et al. Train offline, test online: A real robot learning benchmark. In *2023 IEEE International*
567 *Conference on Robotics and Automation (ICRA)*, pages 9197–9203. IEEE, 2023.
- 568 [74] Tensorflow. TensorFlow Datasets, a collection of ready-to-use datasets. [https://www.tensorflow.](https://www.tensorflow.org/datasets)
569 [org/datasets](https://www.tensorflow.org/datasets).
- 570 [75] J. Pari, N. M. Shafiullah, S. P. Arunachalam, and L. Pinto. The surprising effectiveness of representa-
571 tion learning for visual imitation, 2021.
- 572 [76] J. Ho, A. Jain, and P. Abbeel. Denoising diffusion probabilistic models. *Advances in neural*
573 *information processing systems*, 33:6840–6851, 2020.

574 **A Additional Results**

575 **A.1 10% Bridge Sub-setting**

576 Here we include results for 10% subsetting of the bridge dataset as described in Section 4.4. In the
 577 supplemental material we include videos of rollouts from our experiments.

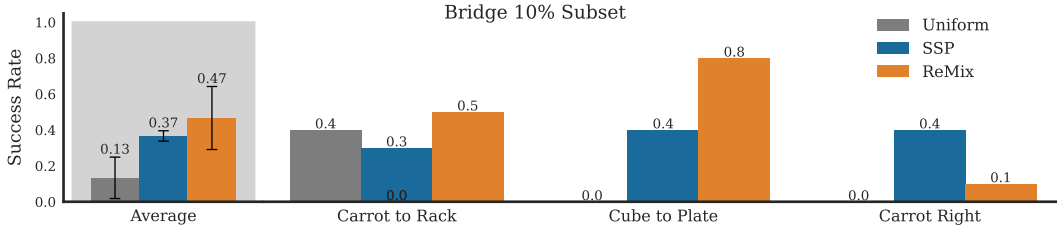


Figure 5: Bridge 10% subsetting.

578 **A.2 Simulation Experiments**

579 We additionally run simulation experiments on the Robomimic NutAssemblySquare task from images
 580 [20]. We chose Robomimic because it was collected using human operators like real world datasets. We
 581 divided the 300 multi-human demonstrations into six domains by operator, which have “better”, “okay”,
 582 and “worse” labels. We run Re-Mix with the same architecture as described in all other experiments, but
 583 train Conditional UNet Diffusion Policies [30] since they performed far better on this benchmark. We
 584 evaluate checkpoints for 100 episodes after 400K training steps. The results are included in Table 3 and
 585 learned Re-Mix weights are shown in Table 4. We can see that the Re-Mix determined weights outperform
 586 uniform weights at both 50% and 25% subsetting. This is likely because Re-Mix up-weights the “better”
 587 operators and comparatively down-weights the “worse” ones. Note that the natural or uniform domain
 588 weights are not even across all operators. This is because some of the operators take longer to complete the
 589 task than others.

Method	50% Subsetting	25% Subsetting
ReMix	77/100	59/100
Uniform	53/100	39/100

Table 3: Performance on the RoboMimic NutAssemblySquare task, divided by operator.

Method	Better 1	Better 2	Okay 1	Okay 2	Worse 1	Worse 2
ReMix	22.8%	20.0%	11.9%	14.6%	18.0%	12.7%
Uniform	9.6%	13.6%	18.7%	14.4%	20.0%	23.7%

Table 4: Domain weights used by Re-Mix in comparison to the natural uniform domain weights.

590 **A.3 Action Distributions**

591 In Fig. 6 we show the action distribution for the BridgeV2 dataset and in Fig. 7 we show the action
 592 distribution for the ToTo dataset, both in log-scale. The BridgeV2 dataset’s action distribution is far more
 593 normal and symmetric than the ToTo action distribution, which is heavily multi-modal and skew. Robust
 594 optimization appears to be more well-behaved on the more normally distributed datasets.

595 **B Dataset Details**

596 **B.1 OpenX RTX Subset**

597 We use a subset of the OpenX Embodiment dataset similar to that used to train the RT-X models [7]. First, we
 598 use the RLDS dataset modification repository (https://github.com/kpertsch/rlds_dataset_mod)
 599 used by Octo Model Team et al. [25] to preprocess the raw datasets downloaded from Tensor Flow

Domain	Uniform Weight	ReMix Weight
0 toykitchen2	0.18728751	0.0961817
1 datacol2_tabletop_dark_wood	0.094527	0.04846529
2 toykitchen1	0.069307	0.07683
3 toykitchen6	0.06940527	0.0573625
4 datacol2_toykitchen7	0.07133783	0.06905
5 datacol2_toykitchen2	0.0432927	0.03651583
6 toykitchen7	0.032803	0.03538789
7datacol2_folding_table	0.038522	0.0809778049
8 datacol1_toykitchen6	0.03606622	0.037404168
9 datacol2_robot_desk	0.025810027	0.034152
10 datacol2_toykitchen6	0.02394393	0.02740302
11 deepthought_folding_table	0.0272809	0.013906823
12 datacol2_laundry_machine laundry_machine	0.02582954	0.0396389
13 datacol2_toykitchen5, toykitchen5	0.0337366	0.049943
14 deepthought_toykitchen2	0.0253313	0.013434348
15 deepthought_robot_desk	0.01978364	0.032410502
16 tabletop_dark_wood	0.0219985	0.024691
17 datacol2_toysink2 toysink2_bww	0.0225748	0.0198516
18 toykitchen2_room8052	0.01083554	0.0295857
19 deepthought_toykitchen1, datacol1_toykitchen1	0.01868	0.04047
20 datacol2_foldtable_tray, minsky_foldtable_tray, datacol2_toykitchen7_tray	0.037856699	0.0484
21 toysink3_bww, toysink3	0.01235829	0.014877
22 datacol2_toykitchen1	0.01155453	0.02194
23 toysink1_room8052 toysink1	0.00979455	0.01831014
24 tool_chest	0.00471524	0.00878
25 toysink5	0.00405418	2.78E-05
26 whiteboard	0.006774	0.0129337
27 toykitchen4	0.00371938	0.00537445
28 toysink4	0.00289793	1.80E-05
29 toykitchen3	0.00124406	2.72E-05
30 realkitchen1_dishwasher	0.00202648	0.000541
31 tabletop_light_wood, tabletop_white, realkitchen1_counter	0.004647549	0.005079152

Table 5: Learned weights by Re-Mix on the Bridge V2 dataset.

600 Datasets [74]. Specifically, we resize all images to 256×256 , and filter the Kuka dataset [72] by an
601 included success key. Note that this does warp images. We use the updated version of the Bridge dataset,
602 available at https://rail.eecs.berkeley.edu/datasets/bridge_release/data/tfds/. The
603 specific composition of the dataset is listed in Table 2. Note that we only train on the primary third-person
604 camera in each dataset. For this reason, we omit the NYU Reacher-grabber dataset [75] which *only* includes
605 wrist cameras. We align all action spaces by converting them to delta cartesian and delta euller angle and
606 binarize all gripper actions.

607 B.2 Bridge V2 Dataset

608 For experiments on bridge-only, we split the bridge dataset into 32 domains. First, we re-downloaded
609 the raw bridge dataset and converted it to RLDS using the DLimp convertor ([https://github.com/
610 kvablack/dlimp/](https://github.com/kvablack/dlimp/)). We then partitioned the bridge dataset by domain using the file path metadata field
611 that lists which setting demonstrations were collected in e.g. “toy-kitchen 1” or “toy-sink-3”. We then
612 manually group the domains into 32 categories. We omitted data that was collected by a scripted policy, as
613 it did not contain the scene information in the filepath metadata. This means we ended up with around
614 45,000 training trajectories, instead of the 60K used in the full bridge dataset. In Table 5 we list the
615 natural weights of each of these domains and the learned weights by Re-Mix. We can see that Re-Mix
616 down-weights some of the largest domains and places their weight on smaller domains.

617 B.3 Co-Training Datasets.

618 Below we describe our co-training data and evaluation procedure for the real-world tasks on the WidowX
619 250 and Franka Panda robots.

620 **WidowX Tasks** We evaluate on a 6-DoF WidowX 250 robot on several new pick place tasks in a toy
621 kitchen setting. Our setup is similar to Bridge V2 [4] with a fixed side camera and a blocking controller.
622 Following Walke et al. [4] we use a blocking controller during evaluation. We collect teleoperated
623 demonstrations using an Oculus Quest Headset for motion tracking and co-train on 25 demonstrations for
624 each of the three tasks “Move Cube out of Sink”, “Move Cup into Sink”, and “Move Fork from Sink to
625 Rack.”

626

627 During evaluation, we examine generalization on various axes. The “Carrot to Rack” task tests generaliza-
628 tion to picking up a new type of target object, “Fork to Rack” tests new unseen object positions, “OOD
629 Cup” tests an object with different shape, “Cube to Plate” and “Cube to Cup” test generalization to new
630 containers, and “Carrot to Right” tests generalization to both a new target object and a new motion. For
631 each of these tasks, we first take a goal image and then evaluate our policies with fixed object locations for
632 up to 100 seconds, stopping early if the robot or objects reach unrecoverable states. For “Carrot to Rack”
633 we do five trials with the carrot facing down and five trials with it facing upwards. For “Fork to Rack” we
634 use an unseen initial position to the right side of the sink and rotate the fork left 45 degrees for five episodes
635 and to the right 45 degrees for the other five.

636 B.4 Franka Tasks

637 We evaluate on a Franka Panda robot on several pick place tasks on a tabletop. We use a fixed over the
638 shoulder camera We co-train on 25 teleoperated demonstrations for each of the tasks “Pen into Cup,” where
639 we put a pen into a cup from 5 different start locations, and “Flip Bowl,” where a bowl is flipped into a
640 drying rack. For the “Pen into Cup” task we use a different pen than in co-training. However, because our
641 franka embodiment with the Robotiq 2F-85 is not found in our pre-training datasets, we evaluate the same
642 tasks as we co-trained on. We evaluate each start location of the pen twice from a new set of predefined
643 positions. As in the WidowX evaluations, we take a goal image for each task and evaluate for up to 100
644 seconds using a 10Hz controller without blocking control.

645 C Training Details

646 **Architecture.** We borrow our architecture from [4] with a few minor changes. Our policies takes as
647 input a history of two consecutive frames and a single goal image and output a sequence of actions via
648 DDPM [76].

649 First, we preprocess all images to fit between -1 and 1. Then, we channel-wise concatenate both the goal
650 image and a grid containing the position of each pixel in (x,y) space also normalized between -1 and 1.
651 Images are then fed to a ResNet 50 encoder, which employs global average pooling on the output to obtain
652 a 512 dimension representation for each image. Both image representations are then concatenated and fed
653 to a diffusion action prediction head.

654 **Hyperparameters.** We use a cosine decay learning rate schedule with an initial learning rate of 0.0002.
655 We train all models for 400K steps and evaluate the final checkpoint, except for Bridge 10% subsetting,
656 which we found to perform better after 200K steps. More detailed hyperparameters are found in Table 6.
657 Note that there are some differences between bridge and RTX which were made for computational reasons
658 – we iterated faster on the bridge dataset before scaling to RTX. We also did maintained aspect ratio for
659 bridge, hence the different image input size, but did not for RTX follow Octo Model Team et al. [25]. We
660 apply data augmentation to all images consistently across the time horizon and goal image (meaning that
661 the goal image and all past images of each example have the same augmentation applied). We use random
662 resize cropping, brightness, contrast, and hue randomization. For k-means in SSP for Bridge we set $k = 32$,
663 equal to the number of domains used for Re-Mix.

	RTX	Bridge
Batch Size	512	384
Action Chunk	4	2
Image Resolution	224×224	224×288

Table 6: Hyperparameters

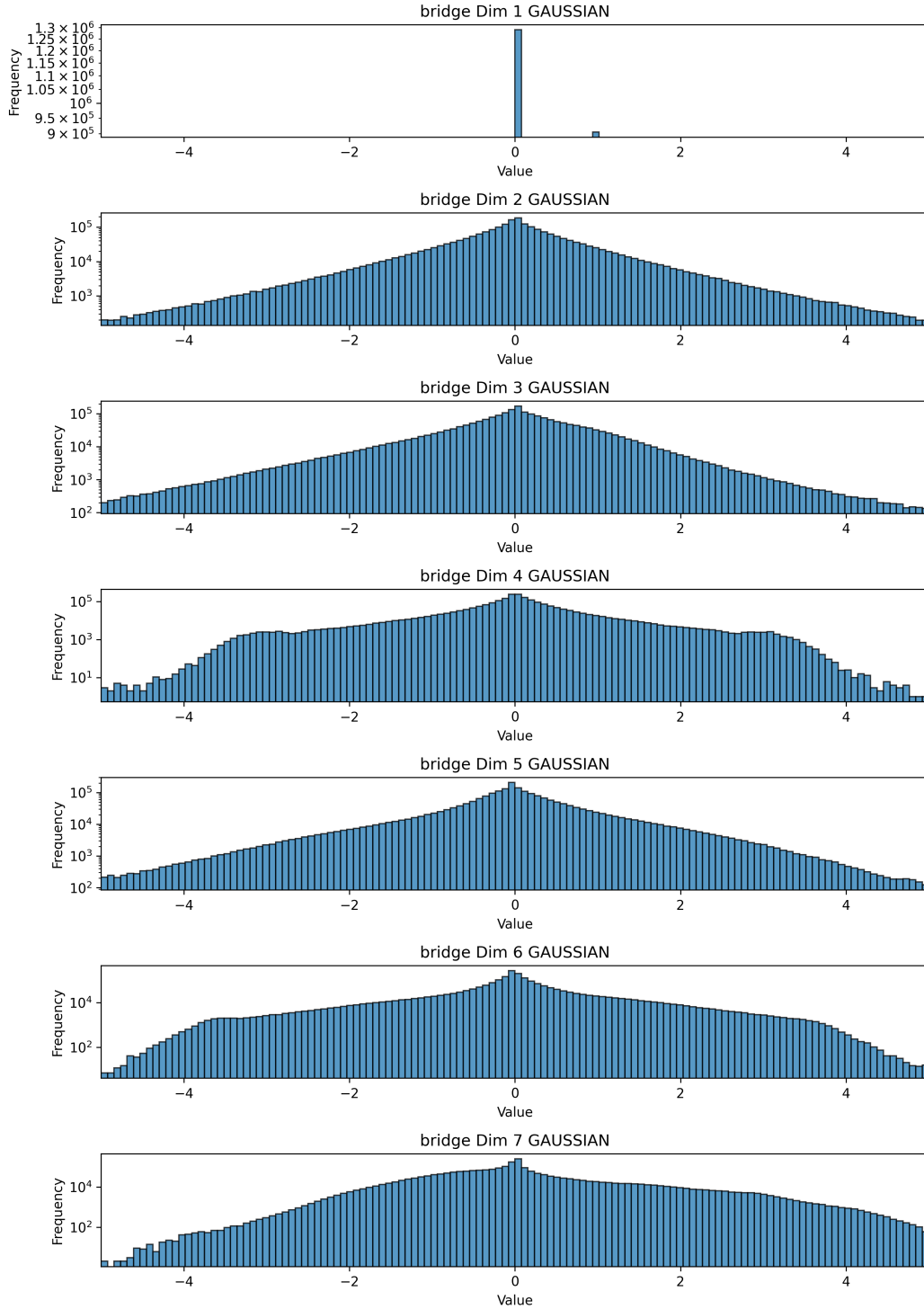


Figure 6: Action distributions for Bridge.

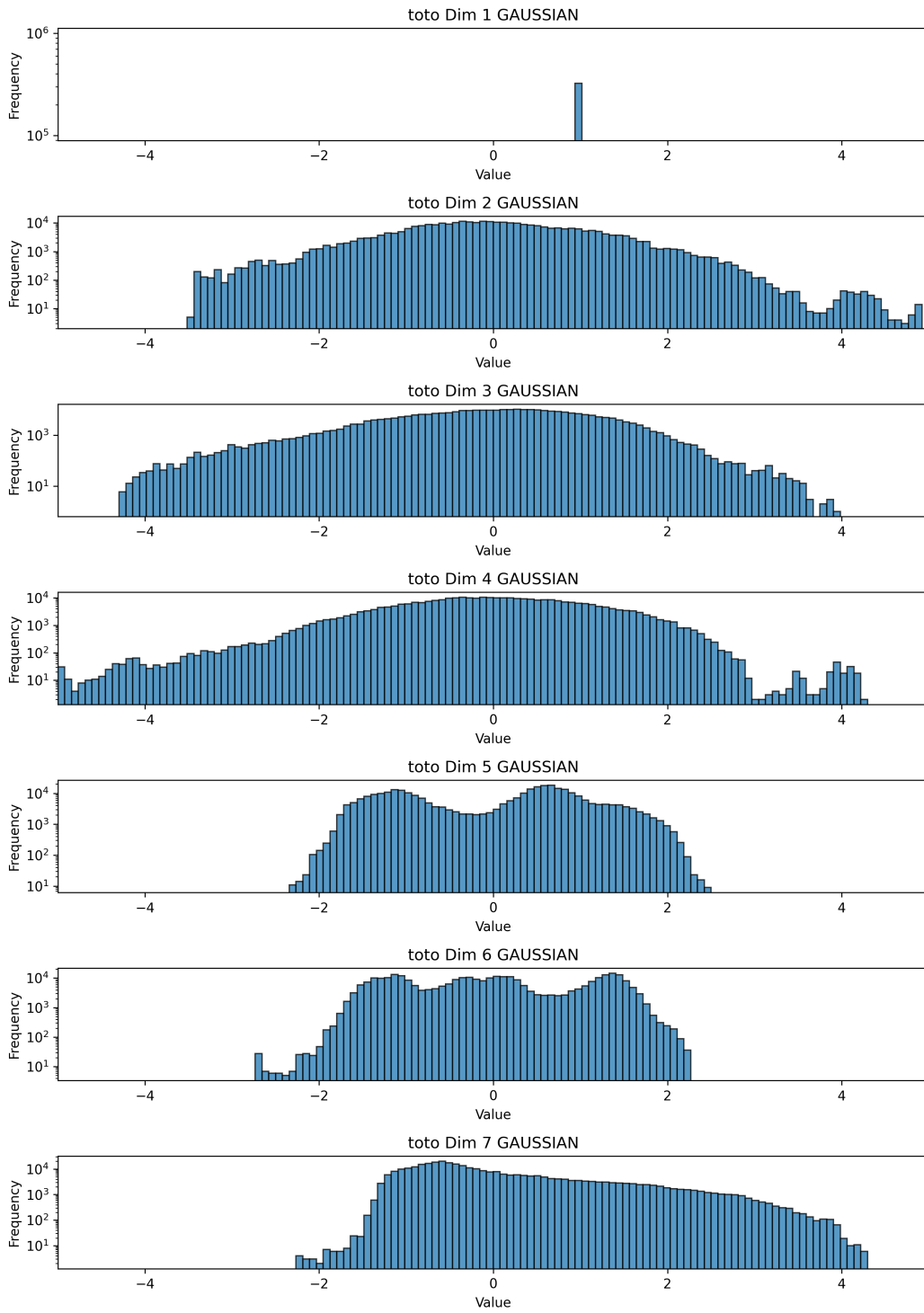


Figure 7: Action distributions for Toto.